Large Molecule Therapeutics

Molecular Cancer Therapeutics

Myostatin Neutralization Results in Preservation of Muscle Mass and Strength in Preclinical Models of Tumor-Induced Muscle Wasting

Rosamund C. Smith, Martin S. Cramer, Pamela J. Mitchell, Andrew Capen, Lysiane Huber, Rong Wang, Laura Myers, Bryan E. Jones, Brian J. Eastwood, Darryl Ballard, Jeff Hanson, Kelly M. Credille, Victor J. Wroblewski, Boris K. Lin, and Josef G. Heuer

Abstract

Skeletal muscle wasting occurs in a great majority of cancer patients with advanced disease and is associated with a poor prognosis and decreased survival. Myostatin functions as a negative regulator of skeletal muscle mass and has recently become a therapeutic target for reducing the loss of skeletal muscle and strength associated with clinical myopathies. We generated neutralizing antibodies to myostatin to test their potential use as therapeutic agents to attenuate the skeletal muscle wasting due to cancer. We show that our neutralizing antimyostatin antibodies significantly increase body weight, skeletal muscle mass, and strength in non–tumor-bearing mice with a concomitant increase in mean myofiber area. The administration of these neutralizing antibodies in two preclinical models of cancer-induced muscle wasting (C26 colon adenocarcinoma and PC3 prostate carcinoma) resulted in a significant attenuation of the loss of muscle mass and strength with no effect on tumor growth. We also show that the skeletal muscle mass– and strength-preserving effect of the antibodies is not affected by the coadministration of gemcitabine, a common chemotherapeutic agent, in both non–tumor-bearing mice and mice bearing C26 tumors. In addition, we show that myostatin neutralization with these antibodies results in the preservation of skeletal muscle mass following reduced caloric intake, a common comorbidity associated with advanced cancer. Our findings support the use of neutralizing antimyostatin antibodies as potential therapeutics for cancer-induced muscle wasting. *Mol Cancer Ther; 14(7); 1661–70. ©2015 AACR.*

Introduction

Cancer cachexia is a multifactorial syndrome defined by an ongoing loss of skeletal muscle mass (with or without loss of fat mass) that cannot be fully reversed by conventional nutritional support and leads to progressive functional impairment (1). Cancer cachexia occurs in 60% to 80% of all patients with advanced cancer and more than 30% of these patients die due to cachexia (2). The presence of cachexia and the associated muscle weakness in these patients reduces the ability to perform activities of daily living and diminishes quality of life. There are no approved drugs for this condition and current therapies are aimed at stimulating appetite or supplementing nutrients in an effort to prevent intake deficits and stabilize weight loss (3). Recent advances in cachexia research have identified several new promising drug targets, including myostatin, a member of the TGFβ superfamily of growth factors highly expressed in skeletal muscle (4). Myostatin was identified as a negative regulator of skeletal muscle mass from the muscle hyperplastic phenotype of naturally occurring hypomorphs and knockout mice (5–7). Furthermore, studies in adult mice demonstrated that reduction or overexpression of myostatin leads to skeletal muscle hypertrophy and atrophy, respectively (8, 9).

Myostatin levels and pathway activation are increased in muscles undergoing atrophy in preclinical models of cancer cachexia (10) as well as in muscles of cancer patients (11). In addition, antisense RNA administration has resulted in less skeletal muscle loss in a preclinical model of cancer cachexia (12). Although antibody-mediated myostatin inhibition has been shown to reduce skeletal muscle loss in several noncancer preclinical models of muscle wasting (13–15), only one previous report describes inhibition in a model of cancer cachexia (16). We report here the preclinical characterization of LSN2478185, a myostatin neutralizing mouse IgG1 monoclonal antibody and its derivative LY2495655, a humanized neutralizing monoclonal antibody to myostatin that can significantly attenuate loss of skeletal muscle mass and function associated with tumor burden. In addition, we present data on the effect of antibody-mediated myostatin neutralization in the context of both chemotherapy and reduced caloric intake, which are two factors that can contribute to the development of muscle wasting in cancer patients.

Lilly Research Laboratories, Eli Lilly and Company, Lilly Corporate Center, Indianapolis, Indiana.

Note: Supplementary data for this article are available at Molecular Cancer Therapeutics Online (http://mct.aacrjournals.org/).

Corresponding Author: Rosamund C. Smith, Lilly Research Laboratories, Eli Lilly and Company, Lilly Corporate Center, Indianapolis, IN 46285. Phone: 317-277-5229; Fax: 317-277-2934; E-mail: smith_ros@lilly.com

doi: 10.1158/1535-7163.MCT-14-0681

Materials and Methods

Recombinant myostatin protein and antibodies

Recombinant human myostatin was either purchased commercially (R&D Systems) or produced in Chinese Hamster Ovary (CHO) cells in a manner similar to previously described methods for the homologous protein TGFβ (17). CHO cells (Lonza; obtained 2004) were passaged and stored frozen in aliquots until needed. Total passage time was less than 6 months. LY2495655 is a humanized IgG4 myostatin antibody derived from LSN2478185, which is a mouse IgG1 antibody. Control IgG antibodies were isotype matched IgG1 or IgG4 with known antigen binding generated within Eli Lilly and Company. Antibodies were stored at 4°C and diluted with 1× PBS pH 7.4 (Invitrogen, Gibco) before injection.

Binding affinity measurements

Myostatin binding affinity measurements were performed using a KinExa 3000 instrument (Sapidyne Instruments; ref. 18). Purified myostatin was immobilized via free amine groups to NHS-activated Sepharose 4 Fast Flow beads (GE Healthcare) at a level of 50 μg/mL of packed beads. Equilibrium binding affinity experiments were performed using 24 analytical cycles, consisting of 12 duplicates. Each cycle was performed at a flow rate of 250 μL/minute during sample injection. A CY5-labeled, rabbit anti-mouse $F(ab')_2$ (Jackson ImmunoResearch) and a CY5-labeled goat anti-human Fcγ (Jackson ImmunoResearch) were used for detection of LSN2478185 and LY2495655, respectively. Concentrations of antibodies ranged from 1 to 20 pmol/L and myostatin concentrations ranged from 0.98 pmol/L to 2 nmol/L. For all experiments, antibody/myostatin mixtures were prepared in the sample buffer and incubated for 4 to 30 hours before measurements. Resulting data were fit to a simple 1:1 binding model using the KinExa instrument software to determine both the binding affinity (K_d) and active antibody concentration. Since mouse and human mature myostatin have identical amino acid sequences, the affinities of the antibodies to mouse myostatin are identical to those for human myostatin.

In vitro cell-based assay

A plasmid containing the SMAD binding element (SBE) repeat (19) driving expression of a luciferase reporter was constructed by cloning of a synthesized SBE repeat sequence (GeneArt, Life Technologies, Inc.) into the NheI-HindIII sites of the pGL3-basic vector (Promega Biotec). HEK-293 cells (ATCC; obtained 2003–2004) were passaged and stored frozen in aliquots until needed. Total passage time was less than 6 months. Cells were maintained in DMEM (Life Technologies) with 10% FBS and antibiotics (Life Technologies). HEK-293 cells were seeded into interior 60 wells of 96-well PDL plates (BioCoat) at 25,000 cells/well. After overnight attachment, the cells were transfected with the reporter construct using Lipofectamine 2000 (Invitrogen) transfection reagent and Opti-MEM medium (Life Technologies) according to manufacturer instructions. After 16 to 20 hours, cells were treated with 50 μL/well of DMEM + 5% dialyzed FBS containing no antibody, a dose range of 0.02–20 μg/mL LSN2478185 or LY2495655, or control IgG antibody. Myostatin protein was added at 2 nmol/L in DMEM + 5% dialyzed FBS, 50 μL/well for a final concentration of 1 nmol/L myostatin and 0.01–10 μg/mL antibody and incubated for 24 hours and then the treatment medium was aspirated. Glo Lysis Buffer (Promega) was added at 75 μL/well, and the plates were stored at −20°C until the time of assay. The plates were thawed at room temperature in a plate shaker for 30 to 60 minutes, 70 μL lysate from each well was combined with 70 μL of Bright Glo Substrate (Promega) in opaque white plates, and light units were measured in a luminometer (Victor). Data were analyzed and graphed with Prism GraphPad software.

Care and use of laboratory animals

All animal studies were conducted in accordance with the American Association for Laboratory Animal Care institutional guidelines. All *in vivo* experimental protocols were approved by the Eli Lilly and Company animal care and use committee.

Pharmacokinetic analysis

Pharmacokinetic analyses for LY2495655 were conducted in female CB17 SCID mice (17–19 grams; Harlan) after a single subcutaneous dose of 1 or 5 mg/kg. Blood samples were collected via cardiac puncture from two animals per treatment group/time point at 6, 12, 24, 48, 72, 120, 168, 240, and 336 hours after administration. Blood (approximately 1 mL) was allowed to clot at room temperature. Serum was prepared by centrifugation and stored frozen at −80°C until assayed. Concentrations of LY2495655 in mouse serum were determined using an antigen capture ELISA assay. Each well of an Immulon 4 microtiter plate (Thermo Fisher Scientific) was coated with myostatin protein (100 μL of 1 μg/mL solution) at 4°C overnight. After washing and blocking (PBS/Casein), standards and samples in 100% serum were added to the wells in a volume of 0.1 mL and were incubated for 1 hour at room temperature. After washing, the bound antibodies were detected with 0.1 mL of a 1:5,000 dilution of HRP-conjugated mouse anti-human light-chain antibody (Southern Biotechnology Associates) and incubated for 1 hour. Samples were developed using the TMB peroxidase substrate system (KPL), detection wavelengths 450 to 630 nm. All incubation steps were performed at room temperature unless noted otherwise. Wash solution was PBS (pH 7.4) and blocking solution was PBS/1%casein. The LY2495655 standards were prepared in mouse serum using a standard curve range of 1.56 to 100 ng/mL and the lower limit of quantitation was defined as 4 ng/mL. Pharmacokinetic parameters were calculated using the WinNonlin Professional software package (version 3.2; Pharsight). Serum concentration–time data were calculated using a model-independent approach based on the statistical moment theory. The pharmacokinetic parameters are presented as a mean across two mouse studies. A pharmacokinetic study of LSN2478185 was conducted in male CD-1 mice (18—20 g) at a single subcutaneous dose of 1 mg/kg following the same protocol (animal number, sample collection, time points) as described for LY2495655. The analytical method was the same as described with the exception that captured antibody was detected with a HRP-conjugated goat anti-mouse IgG (Southern Biotechnology Associates).

Animal experimentation and tumor models

Female or male CB17 SCID mice (17–19 grams) were purchased from Harlan or Taconic. Female BALB/c mice (18–20 g) and male BALB/c mice (23–25 g) were purchased from Harlan. Antibodies were injected subcutaneously in a volume of 0.5 mL.

Body composition data were acquired using quantitative NMR (qNMR) with a Bruker MQ10 NMR Analyzer. Grip strength measurements (in Newtons) were acquired with a digital Grip Strength Meter (Columbus Instruments Model 0167-004L). Four-limb measurements were acquired in the tension peak (C PEAK) mode. The average of 3 readings was recorded. Wet muscle weights were normalized to either brain weight or body weight or recorded directly as muscle weights in mg.

Two milligrams gemcitabine was dosed intraperitoneally in 0.5 mL PBS (Gibco BRL). For a 20 g mouse, this dose of gemcitabine is 333 mg/m^2 and approximates the human dose of 1,000 mg/m^2/week when given three times a week (20). Serum was analyzed for creatinine kinase on a Roche Hitachi Modular Analytics P analyzer with the appropriate reagents by Roche.

In caloric restriction experiments, male BALB/c mice were fed *ad libitum* and food consumption was determined for each mouse. Mice were then randomized into 4 groups by body weight and 2 groups were assigned to an *ad libitum* normal diet. The other two groups were assigned to a restriction of 90% of the *ad libitum* food intake measured from the previous week. Once food restricted animals had lost about 3% to 5% of their initial body weight, both groups were randomized by body weight into equivalent groups for dosing.

Tumor-induced muscle wasting models included murine colon 26 adenocarcinoma (C26) and human prostate tumor PC3 cells. Cells (ATCC; C26 obtained March 2005; PC3 obtained July 2005) were passaged and stored frozen in aliquots until needed. Total passage time was less than 6 months. Cells were grown in DMEM F12 media supplemented with 10% FBS and 1% penicillin/streptomycin (Invitrogen). One or 2 million C26 or 5 million PC3 tumor cells were injected subcutaneously in 0.2 mL PBS in the right flank of female or male SCID mice, respectively. Tumor growth was monitored with electronic calipers by measuring both the length and width of tumors and data. Tumor volume was calculated by the formula: $V = (l \times w^2)/2$. C26 tumors and PC3 cells did not express detectable myostatin RNA (unpublished observations).

Morphometric analysis of muscle

The gastrocnemius (10/group) was collected in 10% neutral buffered formalin and trimmed to obtain sections in three sites: proximal, in the middle of the muscle and distal in an orientation to obtain cross sections of the myofibers. The tissues were embedded in paraffin, sectioned, and stained with hematoxylin and eosin (H&E). Images of the stained sections were collected with an Aperio ScanScope and the image files were processed in Image Pro Plus to collect myofiber cross-section area (CSA; a freehand drawn polygon best fitting the fiber cross-sectional shape) in pixels. Myofibers were selected for measurement by an area-weighted random sampling scheme. Six to 23 myofibers per muscle section per animal (three sections per animal) were analyzed for each treatment group. Each outcome was compared across treatment groups by a mixed model ANOVA with treatment group as a fixed effect, and animal, section, and fiber as random effects. As the results met an O'Brien-Fleming ($P < 0.005$) and Bonferroni ($P < 0.025$) interim analysis cutoff, no further sampling was undertaken. All analysis was conducted in JMP version 5.1 software.

Statistical analysis

Data were analyzed statistically by ANOVA or ANCOVA analysis and a Student unpaired *t* test with JMP 5.1.1 software (SAS institute). Statistical outliers were removed if detected and data were log transformed for analysis. A *P* value of < 0.05 was considered statistically significant.

Results

LSN2478185 and LY2495655 bind myostatin with high affinity and are potent inhibitors of myostatin activity *in vitro*

LSN2478185 is an affinity optimized mouse IgG1 antibody that was obtained by immunization of mice with human myostatin protein. LY2495655 is a genetically engineered humanized version of LSN2478185 on a human IgG4 backbone. The affinity K_d of LSN2478185 to myostatin is 40.0 pmol/L while the affinity K_d of LY2495655 to myostatin is 1.9 pmol/L as determined by KinExa. Both LSN2478185 and LY2495655 neutralized 1 nmol/L human myostatin in a cell-based SBE reporter luciferase assay with IC_{50}s ranging from 0.4 to 1.3 nmol/L (Supplementary Fig. S1).

Pharmacokinetic properties of LSN2478185 and LY2495655 in mice

Antibody pharmacokinetic profiles were determined following a single subcutaneous dose of LSN2478185 at 1 mg/kg in female CD-1 mice or 1 and 5 mg/kg of LY2495655 in SCID mice (Table 1). LSN2478185 and LY2495655 reached maximal plasma concentrations at 12 hours and 24 to 48 hours postdose, respectively. After reaching maximal concentrations, LSN2478185 and LY2495655 cleared with a $t_{1/2}$ of 1.4 days and 4 to 6 days, respectively, supporting once a week administration in the preclinical mouse models.

LSN2478185 dose dependently promotes increased skeletal muscle mass and strength in non–tumor-bearing mice

LSN2478185 or a control IgG was administered at 10 mg/kg as a single dose or as two weekly doses to female BALB/c mice. Both treatment paradigms were able to significantly increase body weight after one week (Fig. 1A) and qNMR lean mass (Fig. 1B) as well as quadriceps weight (Fig. 1C) by 2 weeks relative to the control IgG group. Grip strength was increased only when two weekly doses were given (Fig. 1D; $P < 0.005$), so weekly dosing was used in future experiments.

To examine the dose responsiveness of LSN2478185 on muscle mass over a monthly period, the antibody was administered at doses of 1, 2.5, and 5 mg/kg/wk to female BALB/c mice. The 2.5 and 5 mg/kg dose levels significantly increased body weight

Table 1. Pharmacokinetic properties of anti-myostatin antibodies after subcutaneous administration to mice[a,b]

Antibody	Dose (mg/kg)	T_{max} (h)	C_{max} (μg/mL)	AUC (μg.h/mL)	$t_{1/2}$ (d)	CL (mL/h/kg)
LSN2478185[a]	1	12	4.6	384	1.4	2.6
LY2495655[b]	1	24	6.3	624	4.2	1.4
LY2495655[b]	5	48	46.5	6,143	5.5	0.5

Abbreviations: AUC, area under the serum concentration curve from 0 to 336 hours; C_{max}, maximal serum concentration; CL, clearance; $t_{1/2}$, elimination half-life; T_{max}, time to maximal serum concentration.

[a]Male CD-1 mice.

[b]Female CB17 SCID mice.

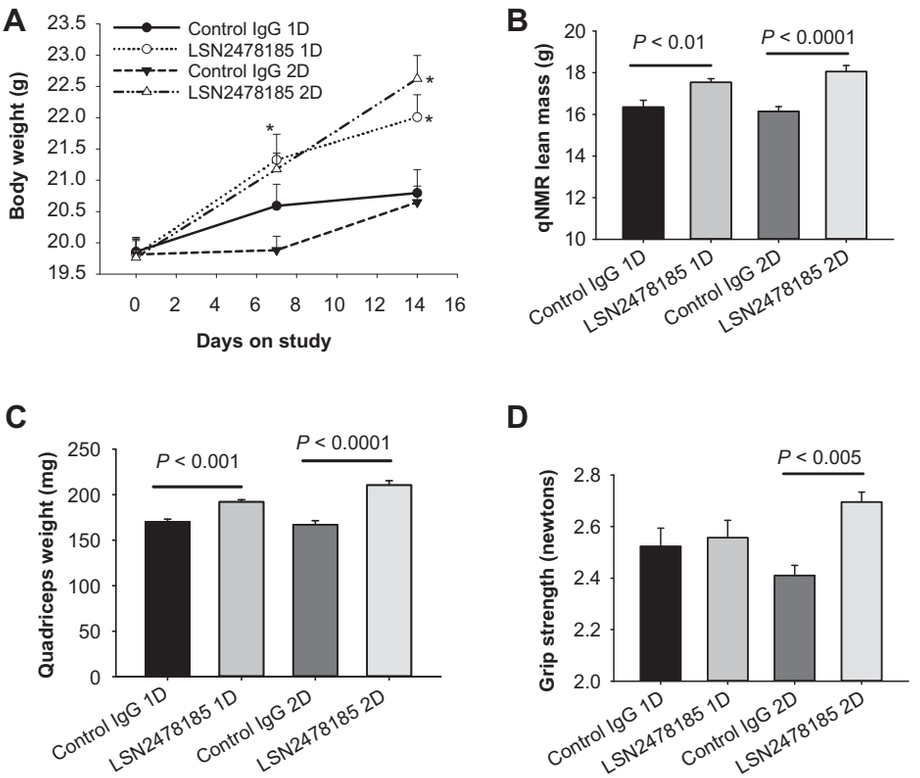

Figure 1.
Effects of LSN2478185 dose frequency on body weight, muscle mass, and strength in non–tumor-bearing mice. Data shown represent the mean ± SEM for body weight (A), qNMR whole body lean mass (B), quadriceps weight (C), and grip strength (D) from female BALB/c mice treated subcutaneously with either a single dose (1D) or two weekly doses (2D) of LSN2478185 or a control IgG at 10 mg/kg for a total of 2 weeks ($n = 8$ mice/group). *, $P < 0.05$, significant relative to the respective control IgG group; ns, not significant.

(Fig. 2A; $P < 0.001$) and qNMR lean mass (Fig. 2B; $P < 0.001$) relative to the control IgG or the 1 mg/kg dose, and significantly increased quadriceps muscle weight relative to the control IgG (Fig. 2C; $P < 0.01$ and < 0.001, respectively). Serum LSN2478185 levels (Fig. 2D) were significantly correlated with quadriceps weight ($r = 0.7$; $P < 0.001$; Fig. 2E).

LSN2478185 builds muscle mass in the presence of gemcitabine

As antimyostatin antibody therapy for cancer-associated muscle wasting might be used concurrently with chemotherapy, we examined the pharmacodynamic activity of LSN2478185 in the presence of gemcitabine. The effects of gemcitabine on C26 tumor growth in mice have already been characterized (20) and gemcitabine is used in pancreatic cancer patients which show muscle wasting in advanced stages (21). Female BALB/c mice were given vehicle or gemcitabine on days 0, 3, 6, 9, and 12. A control IgG or LSN2478185 was administered at 10 mg/kg/wk beginning on day 0 and the experiment was terminated after 3 weeks. Gemcitabine treatment resulted in decreased food consumption only in the control antibody group after the first week (Supplementary Fig. S2A). As expected, LSN2478185 significantly increased body weight (Supplementary Fig. S2B; $P < 0.05$) and gastrocnemius and quadriceps weight relative to the control IgG in the absence of gemcitabine (Supplementary Fig. S2C; $P < 0.005$ and <0.0005, respectively). Addition of gemcitabine did not significantly affect any of the muscle parameters relative to the LSN2478185 treatment or control IgG group, although there was an insignificant decrease in body weight as early as 3 days after administration that recovered by day 20 in the IgG control group (Supplementary Fig. S2B). Neutrophil counts were significantly lower relative to the vehicle groups in both gemcitabine-treated groups at day 13 (Supplementary Fig. S2D; $P < 0.005$). The lack of remarkable findings in a histopathologic assessment of the gastrocnemius muscle as well as the lack of any significant differences in serum creatinine kinase between the groups (data not shown) suggested no muscle damage was incurred by antibody treatment.

LSN2478185 preserves skeletal muscle mass under conditions of reduced caloric intake

A common side effect of standard chemotherapy for cancer patients is appetite suppression resulting in reduced caloric intake, which is a concern in the primary care of these patients. Caloric restriction has been shown to induce the loss of skeletal muscle tissue in elderly men and women (22). To determine whether LSN2478185 could attenuate the loss of skeletal muscle and strength under conditions of reduced caloric intake, male BALB/c mice were either fed *ad libitum* or placed on caloric restriction until weight loss was evident and then treated with antibodies. Body weights for animals fed *ad libitum* ($n = 20$) progressively increased, gaining about 6% of their original body weight on average over a 3-week period from the start of the study (Supplementary Fig. S3A). Over the same period of time, animals placed on the caloric restricted diet ($n = 20$) lost 2% to 5% of their initial body weight (Supplementary Fig. S3A). At this time, animals from both groups were randomized into 2 equivalent groups (10/group) by body weight and dosing with antibodies was initiated. Treatment of the *ad libitum* fed group with LSN2478185 resulted in a trend for increased body weight relative to the control IgG *ad libitum* group that reached

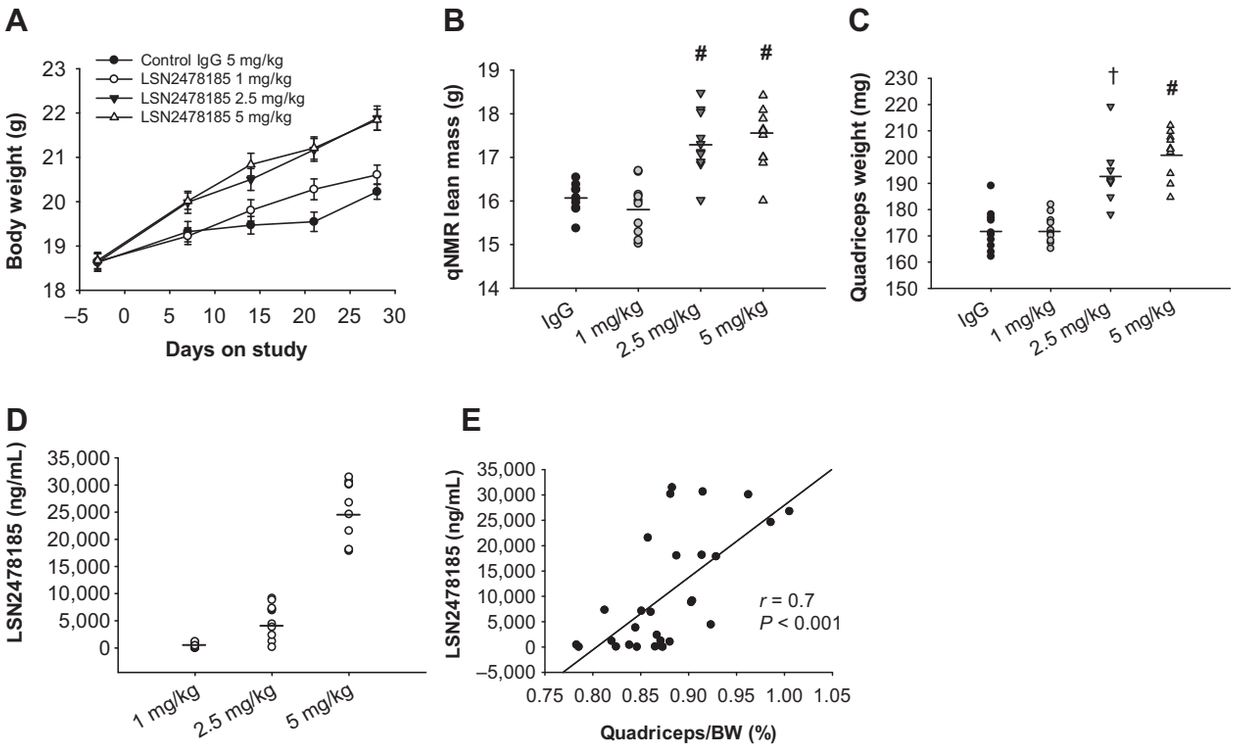

Figure 2.
LSN2478185 dose dependently increases body weight and muscle mass in naïve mice. Data shown for body weight (A), qNMR whole body lean mass (B), quadriceps weight (C), serum values of LSN2478185 at termination (D), 7 days after last dose administration, and a regression plot of normalized quadriceps weight to serum LSN2478185 values (E), after 4 weeks of dosing with LSN2478185 once weekly for 4 weeks in female BALB/c mice at 3 different dose levels ($n = 10$/group). Data shown for body weight represent the mean ± SEM at each time point. Data shown for all other parameters represent individual values with solid horizontal bars representing the mean of each group. #, $P < 0.001$ versus control IgG; †, $P < 0.01$ versus control IgG.

significance by the end of the study with 10.7% greater body weight than the control IgG group (Supplementary Fig. S3A; $P < 0.05$). Animals on the caloric restricted diet continued to lose body weight over the next 4 weeks, with no significant difference between the control IgG and LSN2478185-treated groups (Supplementary Fig. S3A). Animals on an *ad libitum* diet treated with LSN2478185 had no effect on whole body fat mass compared with the control IgG group (Supplementary Fig. S3B) but showed significant increases in qNMR lean mass (Supplementary Fig. S3C; $P < 0.005$) as well as gastrocnemius and quadriceps muscle weights compared with the IgG control group (Supplementary Fig. S3D; $P < 0.01$ and <0.0001, respectively). Animals on the caloric restricted diet treated with the IgG control exhibited significantly less qNMR lean mass (Supplementary Fig. S3C; $P < 0.0001$) as well as less gastrocnemius and quadriceps wet muscle weights (Supplementary Fig. S3D; $P < 0.0001$) compared with the IgG control *ad libitum* group. The IgG control mice on the caloric restricted diet did not lose fat mass relative to the *ad libitum* fed control mice (Supplementary Fig. S3B), suggesting that the majority of the weight loss was due to a loss in lean mass. In comparing the 2 groups on the caloric restricted diet, animals treated with LSN2478185 had significantly less whole body fat mass (Supplementary Fig. S3B; $P < 0.05$) and significantly greater normalized gastrocnemius and quadriceps muscle weights relative to the control IgG group (Supplementary Fig. S3E; $P < 0.05$ and <0.0001, respectively).

LY2495655 builds muscle mass and strength in naïve SCID mice with accompanying muscle fiber hypertrophy and prevents the loss of muscle mass and strength in the C26 tumor model

As LY2495655 is a humanized version of the LSN2478185 antibody and would be the antibody used in clinical testing, we then moved to examining effects of LY2495655 in mouse models. LY2495655 was first tested in female SCID mice as these mice would be used for tumor studies. LY2495655 significantly increased body weight (Fig. 3A), qNMR lean mass (Fig. 3B), individual muscle weights (Fig. 3C), and grip strength (Fig. 3D) relative to an isotype control antibody. Gastrocnemius weights were 10%, 16.5%, and 18% higher on average for the 2, 5, and 10 mg/kg LY2495655 groups, respectively, relative to the control IgG group. Similar results were observed for the quadriceps muscle. The increases in muscle mass were also accompanied by significant increases in grip strength for the 5 and 10 mg/kg groups, which were 8.3% and 7.6% higher than the control IgG group, respectively ($P < 0.005$ and $P < 0.05$).

To determine the ability of LY2495655 to attenuate skeletal muscle wasting associated with cancer, we used the C26 tumor model of muscle wasting that has been shown to secrete myostatin protein (23). We tested the antibody at 10 mg/kg/wk in female SCID mice with initiation of treatment at 6 days after tumor cell injection. Non–tumor-bearing animals were included as controls. C26 tumors grew progressively over time

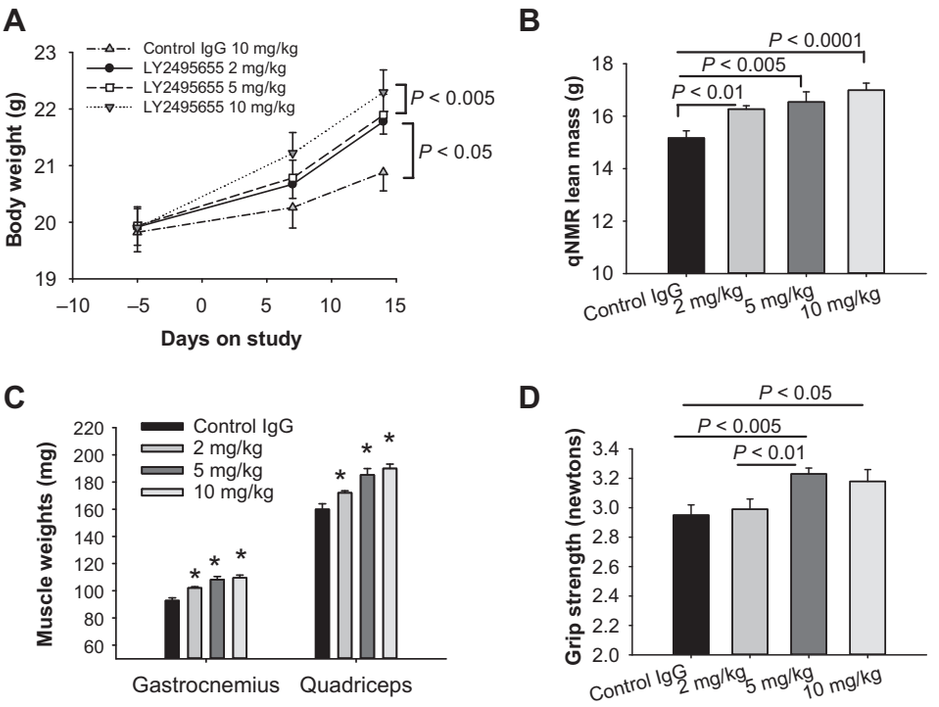

Figure 3.
LY2495655 increases body weight, muscle mass, and strength in naïve SCID mice. Data shown represent the mean ± SEM for body weight (A), qNMR lean mass (B), gastrocnemius and quadriceps wet muscle weights (C), and grip strength from female SCID mice (D) treated with multiple dose levels of LY2495655 or 10 mg/kg of a control IgG once weekly for 2 weeks ($n = 10$ mice/group). *, $P < 0.05$, significant relative to the respective control IgG group.

irrespective of treatment (Fig. 4A). Tumor growth in mice that received the control IgG resulted in a significant loss of net body weight (equivalent to body weight minus tumor weight; Fig. 4B; $P < 0.05$), wasting of individual muscles (Fig. 4C; $P < 0.05$) and reduction of grip strength compared with non–tumor-bearing mice (Fig. 4D; $P < 0.0001$). There were two deaths in the control IgG tumor group during the experiment. There was no significant effect of LY2495655 treatment on net body weight in tumor-bearing animals compared with the control IgG tumor group (Fig. 4B). However, LY2495655 treatment preserved individual muscle weights (Fig. 4C; $P < 0.05$) and grip strength (Fig. 4D; $P < 0.05$) relative to the control IgG tumor group.

In tumor-bearing mice receiving the control antibody, a statistically significant decrease of 23% in myofiber CSA occurred compared with non–tumor-bearing animals (Fig. 4E; $P < 0.005$), while there was a 7% nonsignificant increase in myofiber CSA in tumor-bearing animals receiving LY2495655 versus those receiving a control IgG (Fig. 4E). Consistent with earlier results, LY2495655 treatment in non–tumor-bearing animals resulted in significant increases in body weight, gastrocnemius weight, and quadriceps weight (Fig. 4B and C; $P < 0.005$). These mice also exhibited a statistically significant 18% increase of myofiber CSA compared with nontumor animals that were given the control antibody (Fig. 4E, $P = 0.012$), confirming a myofiber hypertrophy effect with LY2495655 treatment.

LY2495655 builds muscle mass in the presence of gemcitabine in both non–tumor-bearing and C26 tumor-bearing mice

We next tested the ability of LY2495655 to attenuate muscle loss and strength in the presence of gemcitabine in the C26 tumor model. Non–tumor-bearing and tumor-bearing female SCID mice were treated with either a control IgG or LY2495655 at 10 mg/kg/wk. Gemcitabine was administered on days 9 and 12 after tumor cell inoculation when tumors were well established and the study was terminated at 14 days after tumor cell inoculation. There were no differences between the groups for tumor growth (Fig. 5A). Food consumption measured during the last week of the study was decreased on a per mouse basis in both tumor-bearing groups relative to the non–tumor-bearing group, whereas the LY2495655-treated tumor group consumed more food than the control IgG tumor group (Fig. 5B). At the time of gemcitabine initiation, only the tumor-bearing control IgG animals showed weight loss from baseline (Fig. 5C). Gemcitabine treatment prevented further tumor growth in both treatment arms (Fig. 5A), yet did not result in complete tumor regression. Even though tumor growth had stopped from day 9 to 14 after tumor cell injection, net body weight loss continued in both tumor groups albeit significantly less in the LY2495655-treated group (Fig. 5C; $P < 0.05$). Analysis of muscle and grip strength in the tumor-bearing treatment groups indicated that LY2495655 treatment resulted in significantly greater grip strength (Fig. 5E; $P < 0.05$) and muscle mass, measured either by qNMR (Fig. 5D; $P < 0.005$) or from normalized muscle weights for quadriceps and diaphragm (SupplementaryFig. S4A and S4B; $P < 0.0001$ and 0.0005, respectively). The nontumor group treated with LY2495655 showed significant increases in normalized quadriceps and diaphragm muscle weights (SupplementaryFig. S4B; $P < 0.001$ and 0.05, respectively). There were also increases in body weight (Fig. 5C), qNMR lean mass (Fig. 5D), and grip strength (Fig. 5E). There was no significant effect of LY2495655 on heart weight in either nontumor or tumor groups (Supplementary Fig. S4C).

LY2495655 administration attenuates the loss of body weight, muscle mass, and strength in the PC3 tumor model

LY2495655 was tested in a PC3 tumor xenograft model that has much slower onset and kinetics of body weight loss

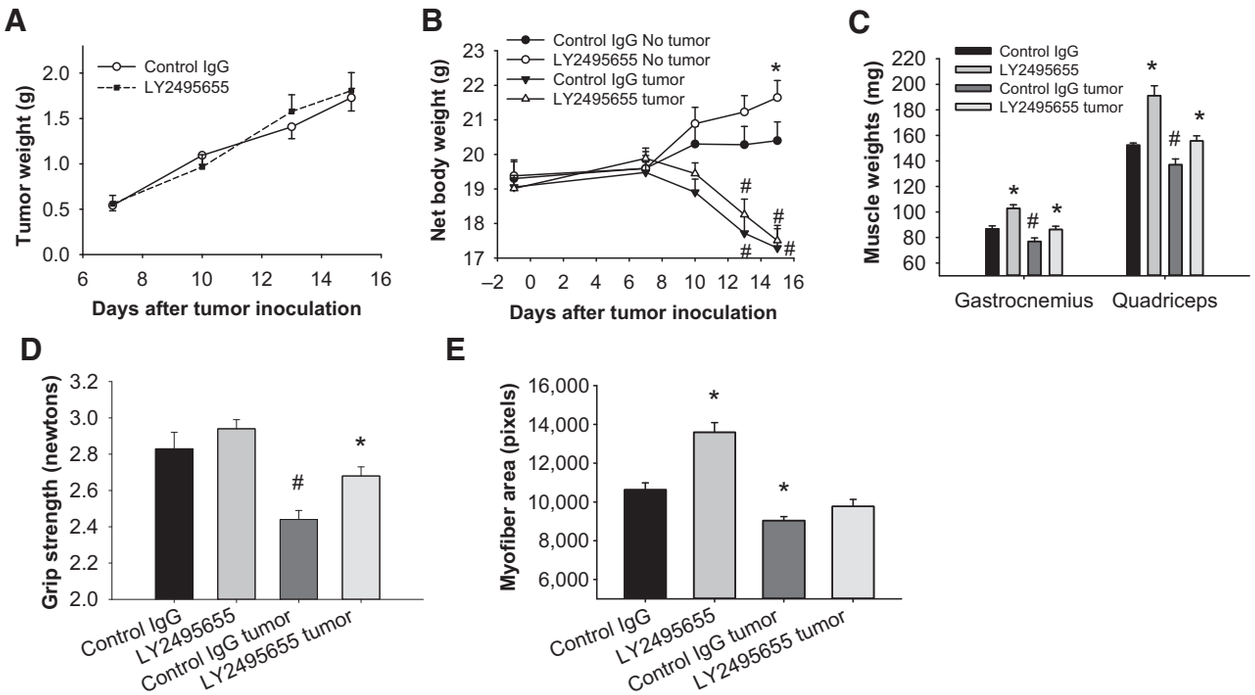

Figure 4.
LY2495655 reduces the loss of muscle mass and strength in C26 tumor-bearing mice. Data shown represent the mean ± SEM for tumor growth (A), net body weight (B), gastrocnemius and quadriceps muscle weights (C), grip strength (D), and cross-sectional myofiber area in female SCID mice (E) with ($n = 13$–15 mice/group) or without ($n = 10$/group) C26 tumors and treated with either a control IgG or LY2495655 at 10 mg/kg once weekly for 2 weeks. *, $P < 0.05$, significant relative to the respective control IgG group; #, $P < 0.05$, significant relative to the control IgG no tumor group.

than the C26 tumor model. The implantation of PC3 tumor cells into male SCID mice resulted in progressive tumor growth (Supplementary Fig. S5A) that resulted in a significant loss of body weight (Supplementary Fig. S5B; $P < 0.05$), qNMR lean mass (Supplementary Fig. S5C; $P < 0.0001$), and grip strength (Supplementary Fig. S5D; $P < 0.0001$) compared to non–tumor-bearing SCID mice. There was a significant association of grip strength with qNMR lean mass (Supplementary Fig. S5E; $P < 0.001$).

LY2495655 or a control IgG was initiated one day after PC3 tumor cell inoculation into male SCID mice and dosed at 10 mg/kg/wk to day 52 ($n = 14$/group). All mice survived to the endpoint of 52 days. Tumors grew progressively in both groups with no difference between the 2 groups (Fig. 6A). In tumor-bearing animals, body weight loss was apparent in the control IgG tumor group by day 24 relative to the nontumor control IgG group and became progressively greater with time (Fig. 6B). Treatment of tumor-bearing animals with LY2495655 resulted in significantly less body weight loss relative to the tumor control group at day 52 (Fig. 6B; $P < 0.0001$). While the tumor control group exhibited significant wasting of diaphragm, gastrocnemius, and quadriceps muscles relative to the control no tumor group (Fig. 6C; $P < 0.0001$), treatment with LY2495655 resulted in significant attenuation of muscle wasting as all muscle weights were not significantly different from the control nontumor group and were significantly greater than the control tumor group (Fig. 6C; $P < 0.0001$). The muscle weights were normalized to brain weight and brain weights were not different between groups (Supplementary Fig. S6A). Normalized muscle weights in the LY2495655 tumor group were also significantly greater than those in the tumor-bearing control group (Supplementary Fig. S6B; $P < 0.0001$). In tumor-bearing animals, the increase in muscle weights seen with LY2495655 treatment resulted in a concomitant significant increase in grip strength compared with the control tumor group (Fig. 6D $P < 0.005$) while grip strength in the control tumor group was significantly less than the non-tumor group (Fig. 6D; $P < 0.0001$). Consistent with previous experiments, treatment with LY2495655 in non–tumor-bearing mice resulted in significant increases in muscle weights relative to the control IgG group (Fig. 6C; $P < 0.005$) and also in normalized muscle weights (Supplementary Fig. S6B; $P < 0.0001$).

Discussion

There are currently no approved drugs to treat skeletal muscle wasting associated with cancer cachexia and this condition represents a significant unmet medical need as it contributes to the morbidity and mortality of cancer patients. Myostatin has emerged as a rational drug target to inhibit the muscle wasting that occurs with chronic illnesses, including cancer. We report here the preclinical characterization of a humanized antibody with high affinity for myostatin that is currently under clinical evaluation for muscle wasting associated with cancer and other disorders (24, 25). LY2495655 was able to rapidly increase not only body weight and skeletal muscle mass, but also muscle strength in naïve young adult mice in a dose-dependent manner, consistent with previous reports of myostatin antibodies (8, 14). The observed increase in skeletal muscle fiber hypertrophy and the

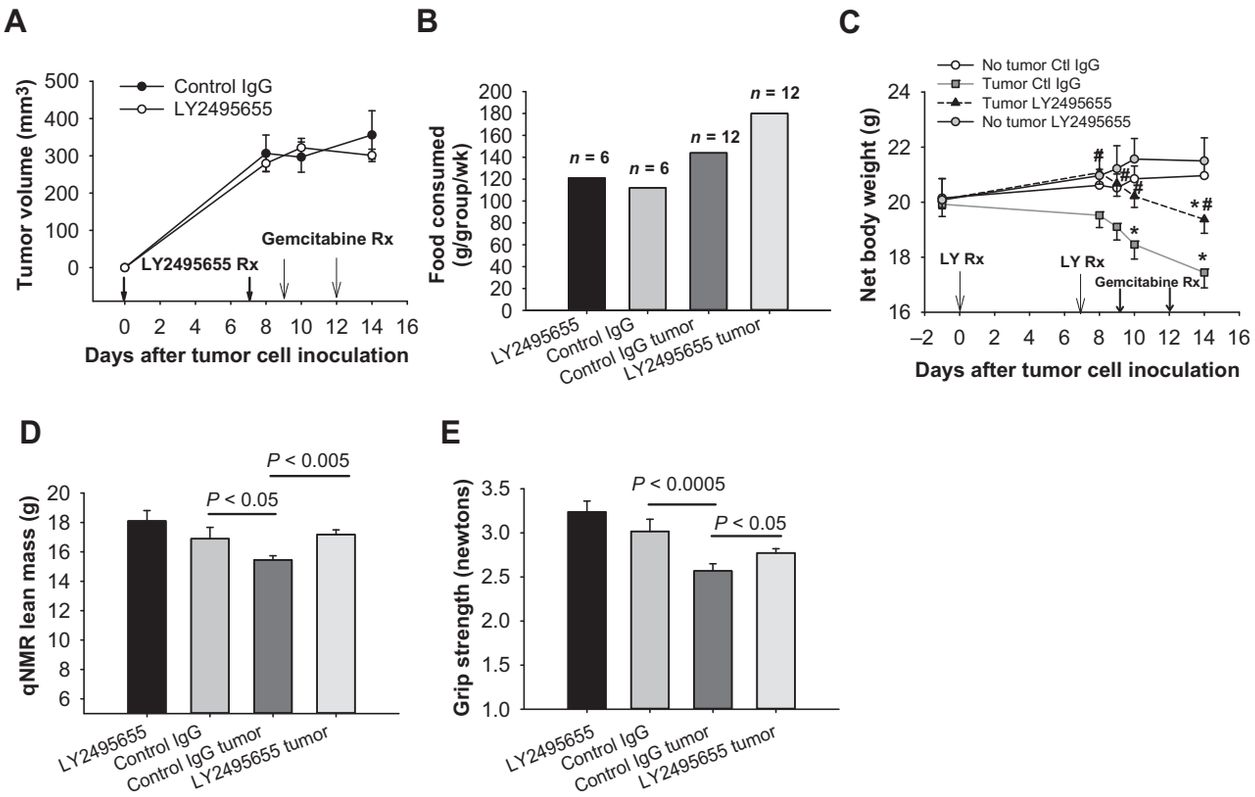

Figure 5.
LY2495655 increases body weight, muscle mass, and strength in the presence of gemcitabine in SCID mice bearing C26 tumors. Data are shown for tumor growth (A), food consumed per group during the last week (B), net body weight (C), qNMR whole body lean mass (D), and grip strength in SCID mice treated with a control IgG or LY2495655 (E) in the absence ($n = 6$ mice/group) or presence of C26 tumors ($n = 12$ mice/group) treated with gemcitabine. Data represent the mean ± SEM except for food consumed. *, $P < 0.05$, significant relative to the no tumor control IgG group; #, $P < 0.05$, significant relative to the tumor control IgG group.

lack of effect on heart weight with LY2495655 treatment in mice are also consistent with previous reports (8, 26).

LY2495655 antibody was shown to prevent the loss of skeletal muscle mass in two models of cancer-induced skeletal muscle wasting. While the LY2495655 antibody was unable to prevent body weight loss in the C26 model, the treatment did significantly preserve muscle mass and even increased diaphragm weight. This observation is important as the wasting of the respiratory muscles is believed to contribute to the poor prognosis of advanced pancreatic cancer patients with greater than 15% loss of body weight (27). In contrast, LY2495655 treatment in the PC3 model was able to significantly promote body weight gain, and promoted significant increases in skeletal muscle mass. Importantly, in both models, LY2495655 treatment was able to prevent the loss of muscle strength that was associated with muscle wasting. This is important as the loss of muscle strength in cancer cachexia patients is known to significantly contribute not only to the morbidity and mortality of the condition, but also to the quality of life for these patients (28). Our data are also consistent with results from a recent study in which a myostatin antibody was shown to prevent the loss of muscle mass and strength in a Lewis Lung carcinoma tumor model (16).

Cancer patients are often treated with chemotherapy as part of their standard of care. Skeletal muscle atrophy has been associated with increased toxicity to chemotherapeutic agents (27–29). As the intent of chemotherapy is to kill proliferating cells, there was a possibility that the effects of a myostatin antibody might be compromised by chemotherapy and that coadministration of both agents in a cancer setting might not be feasible. The results reported in this study show convincingly for the first time that the effects of a myostatin antibody on muscle mass are unaffected by coadministration of a chemotherapeutic agent with or without tumor. Recent mechanistic studies of myostatin inhibition *in vitro* and *in vivo* have diminished the importance of satellite cell activation and proliferation and highlighted the contribution of an activation of muscle fiber protein synthesis to induction of muscle hypertrophy (30–33), consistent with our results. An ongoing clinical study with LY2495655 in pancreatic cancer patients in the presence of chemotherapeutic agents will determine whether this finding translates to man (25).

Of note, gemcitabine induced a food intake deficit and body weight loss during the first week in nontumor animals as nausea, appetite loss and body weight loss are noted as potential side effects of this drug and many other chemotherapy drugs in cancer patients. Surprisingly, this side effect was not observed in the LSN2478185 plus gemcitabine-treated animals. The mechanism behind this effect is unclear.

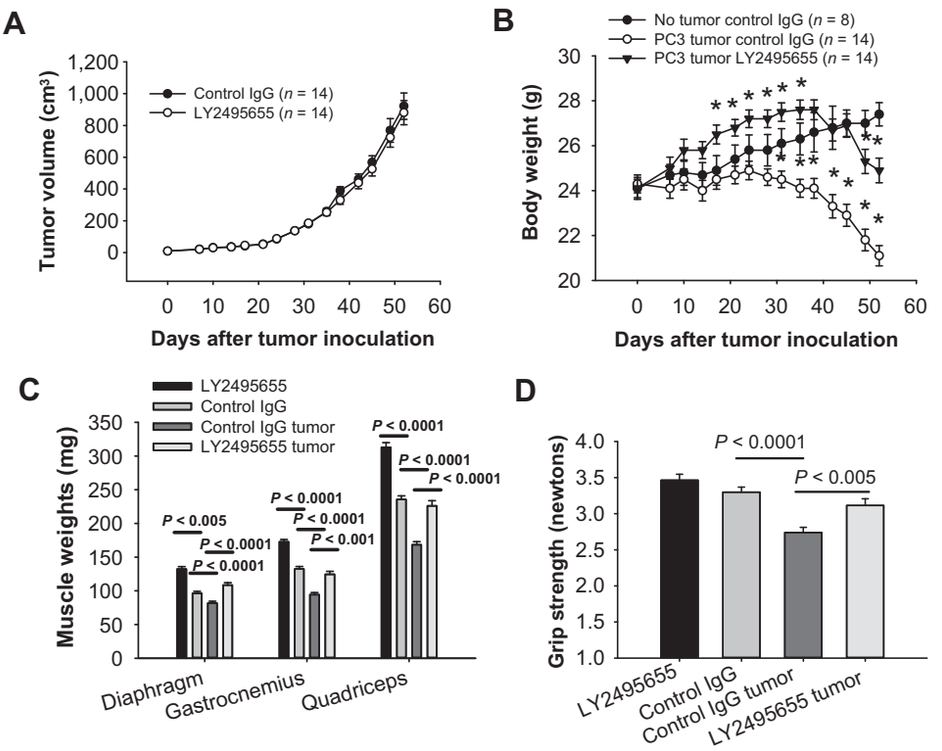

Figure 6.
LY2495655 attenuates loss of body weight, muscle mass, and strength in SCID mice with PC3 tumors. Data represent the mean ± SEM for tumor growth (A), body weight (B), individual muscle weights (C), and grip strength in SCID mice (D) treated with a control IgG or LY2495655 in the absence ($n = 8$ mice/group) or presence of PC3 tumors ($n = 14$ mice/group). *, $P < 0.05$, significant relative to the no tumor control IgG group.

Reduced caloric intake is another key component of cancer cachexia and opposing this is part of the current strategy to treat cachexia in cancer patients through administration of appetite stimulants and nutritional support (34). Myostatin expression has been shown to increase in specific muscles and contribute to muscle atrophy during food deprivation in mice (35). While LSN2478185 treatment under reduced caloric intake was unable to prevent the loss of body weight and whole body muscle mass, the antibody treatment was able to significantly attenuate the loss of muscle mass relative to body weight compared with the control antibody. These data demonstrate the importance of providing necessary food intake in building muscle mass with myostatin inhibition and show that even in conditions where body weight is not affected by myostatin antibody treatment, myostatin inhibition in muscle may have positive effects on whole body lean mass.

In conclusion, our preclinical data reported here from two different models of tumor induced skeletal muscle wasting with a myostatin neutralizing antibody are consistent with the hypothesis that myostatin plays a prominent role in the skeletal muscle wasting associated with cancer and supports the clinical testing of LY2495655 in patients with cancer-associated muscle wasting.

Disclosure of Potential Conflicts of Interest

No potential conflicts of interest were disclosed.

Authors' Contributions

Conception and design: R.C. Smith, M.S. Cramer, K.M. Credille, V.J. Wroblewski, B.K. Lin, J.G. Heuer

Development of methodology: A. Capen, R. Wang, B.J. Eastwood, K.M. Credille, V.J. Wroblewski, J.G. Heuer

Acquisition of data (provided animals, acquired and managed patients, provided facilities, etc.): M.S. Cramer, P.J. Mitchell, L. Huber, K.M. Credille, V.J. Wroblewski, J.G. Heuer

Analysis and interpretation of data (e.g., statistical analysis, biostatistics, computational analysis): R.C. Smith, M.S. Cramer, P.J. Mitchell, B.E. Jones, B.J. Eastwood, J. Hanson, K.M. Credille, B.K. Lin, J.G. Heuer

Writing, review, and/or revision of the manuscript: R.C. Smith, M.S. Cramer, B.E. Jones, D. Ballard, K.M. Credille, V.J. Wroblewski, B.K. Lin, J.G. Heuer

Administrative, technical, or material support (i.e., reporting or organizing data, constructing databases): M.S. Cramer, P.J. Mitchell, L. Myers, B.E. Jones, D. Ballard, J.G. Heuer

Study supervision: R.C. Smith, J.G. Heuer

Other (developed the preclinical model): A. Capen

Acknowledgments

The authors acknowledge and thank Adam Couts and Jaime Schindler who aided in the counting and measurement of the myofibers in the morphometry analysis. The authors also thank Dianna Jaqua, Ganesh Sharma, and Tonghai Zhang for necropsy support and Kelly Coble for pharmacokinetic support.

The costs of publication of this article were defrayed in part by the payment of page charges. This article must therefore be hereby marked *advertisement* in accordance with 18 U.S.C. Section 1734 solely to indicate this fact.

Received August 13, 2014; revised April 6, 2015; accepted April 17, 2015; published OnlineFirst April 23, 2015.

References

1. Fearon K, Strasser F, Anker SD, Bosaeus I, Bruera E, Fainsinger RL, et al. Definition and classification of cancer cachexia: an international consensus. Lancet Oncol 2011;5:489–95.
2. von Haehling S, Anker SD. Cachexia as a major underestimated and unmet medical need: facts and numbers. J Cachexia Sarcopenia Muscle 2010;1:1–5.

3. Dodson S, Baracos VE, Jatoi A, Evans WJ, Cella D, Dalton JT, et al. Muscle wasting in cancer cachexia: clinical implications, diagnosis, and emerging treatment strategies. Annu Rev Med 2011;62:265–79.
4. Roth SM, Walsh S. Myostatin: a therapeutic target for skeletal muscle wasting. Curr Opin Clin Nutr Metab Care 2004;3:259–63.
5. McPherron AC, Lawler AM, Lee SJ. Regulation of skeletal muscle mass in mice by a new TGF-beta superfamily member. Nature 1997;387: 83–90.
6. Mosher DS, Quignon P, Bustamante CD, Sutter NB, Mellersh CS, Parker HG, et al. A mutation in the myostatin gene increases muscle mass and enhances racing performance in heterozygote dogs. PLoS Genet 2007;3: 779–86.
7. Schuelke M, Wagner KR, Stolz LE, Hübner C, Riebel T, Kömen W, et al. Myostatin mutation associated with gross muscle hypertrophy in a child. New Engl J Med 2004;350:2682–8.
8. Whittemore LA, Song K, Li X, Aghajanian J, Davies M, Girgenrath S, et al. Inhibition of myostatin in adult mice increases skeletal muscle mass and strength. Biochem Biophys Res Commun 2003; 300:965–71.
9. Zimmers TA, Davies MV, Koniaris LG, Haynes P, Esquela AF, Tomkinson KN, et al. Induction of cachexia in mice by systemically administered myostatin. Science 2002;296:1486–8.
10. Costelli P, Muscaritoli M, Bonetto A, Penna F, Reffo P, Bossola M, et al. Muscle myostatin signalling is enhanced in experimental cancer cachexia. Eur J Clin Invest 2008;38:531–8.
11. Aversa Z, Bonetto A, Penna F, Costelli P, Di Rienzo G, Lacitignola A, et al. Changes in myostatin signaling in non-weight-losing cancer patients. Ann Surg Oncol 2012;19:1350–6.
12. Liu CM, Yang Z, Liu CW, Wang R, Tien P, Dale R, et al. Myostatin antisense RNA-mediated muscle growth in normal and cancer cachexia mice. Gene Ther 2008;15:155–60.
13. Murphy KT, Ryall JG, Snell SM, Nair L, Koopman R, Krasney PA, et al. Antibody-directed myostatin inhibition improves diaphragm pathology in young but not adult dystrophic mdx mice. Am J Pathol 2010; 176:2425–34.
14. Murphy KT, Koopman R, Naim T, Léger B, Trieu J, Ibebunjo C, et al. Antibody-directed myostatin inhibition in 21-mo-old mice reveals novel roles for myostatin signaling in skeletal muscle structure and function. FASEB J 2010;24:4433–42.
15. Murphy KT, Cobani V, Ryall JG, Ibebunjo C, Lynch GS. Acute antibody-directed myostatin inhibition attenuates disuse muscle atrophy and weakness in mice. J Appl Physiol 2011;110:1065–72.
16. Murphy KT, Chee A, Gleeson BG, Naim T, Swiderski K, Koopman R, et al. Antibody-directed myostatin inhibition enhances muscle mass and function in tumor-bearing mice. Am J Physiol Regul Integr Comp Physiol 2011;301:R716–26.
17. Archer SJ, Bax A, Roberts AB, Sporn MB, Ogawa Y, Piez KA, et al. Transforming growth factor beta 1: NMR signal assignments of the recombinant protein expressed and isotopically enriched using Chinese hamster ovary cells. Biochemistry 1993;32:1152–63.
18. Darling RJ, Brault PA. Kinetic exclusion assay technology: characterization of molecular interactions. Assay Drug Dev Technol 2004;2: 647–57.
19. Nagarajan RP, Zhang J, Li W, Chen Y. Regulation of Smad7 promoter by direct association with Smad3 and Smad4. J Biol Chem 1999;274: 33412–8.
20. Veerman G, Ruiz van Haperen VW, Vermorken JB, Noordhuis P, Braakhuis BJ, Pinedo HM, et al. Antitumor activity of prolonged as compared with bolus administration of 2′,2′-difluorodeoxycytidine in vivo against murine colon tumors. Cancer Chemother Pharmacol 1996; 38:335–42.
21. Robinson DW Jr, Eisenberg DF, Cella D, Zhao N, de Boer C, DeWitte M. The prognostic significance of patient-reported outcomes in pancreatic cancer cachexia. J Support Oncol 2008;6:283–90.
22. Weiss EP, Racette SB, Villareal DT, Fontana L, Steger-May K, Schechtman KB, et al. Lower extremity muscle size and strength and aerobic capacity decrease with caloric restriction but not with exercise-induced weight loss. J Appl Physiol 2007;102:634–40.
23. Lokireddy S, Wijesoma IW, Bonala S, Wei M, Sze SK, McFarlane C, et al. Myostatin is a novel tumoral factor that induces cancer cachexia. Biochem J 2012;446:23–36.
24. Jameson GS, Von Hoff DD, Weiss GJ, Richards DA, Smith DA, Becerra C, et al. Safety of the antimyostatin monoclonal antibody LY2495655 in healthy subjects and patients with advanced cancer. J Clin Oncol 2012;30 suppl: abstr 2516.
25. Smith RC, Lin BK. Myostatin inhibitors as therapies for muscle wasting associated with cancer and other disorders. Curr Opin Support Palliat Care 2013;7:352–60.
26. Cohn RD, Liang HY, Shetty R, Abraham T, Wagner KR. Myostatin does not regulate cardiac hypertrophy or fibrosis. Neuromuscul Disord 2007;17: 290–6.
27. Eastern Cooperative Oncology Group Dewys WD, Begg C, Lavin PT, Band PR, Bennett JM, Bertino JR, et al. Prognostic effect of weight loss prior to chemotherapy in cancer patients. Am J Med 1980;69:491–7.
28. Donohoe CL, Ryan AM, Reynolds JV. Cancer cachexia: mechanisms and clinical implications. Gastroenterol Res Pract 2011;2011:601434.
29. Basu B, Jodrell D. Progress in pancreatic cancer: moving beyond gemcitabine? Expert Rev Anticancer Ther 2012;12:997–1000.
30. Lee S-J, Huynh TV, Lee Y-S, Sebald SM, Wilcox-Adelman SA, Iwamori N, et al. Role of satellite cells versus myofibers in muscle hypertrophy induced by inhibition of the myostatin/activin signaling pathway. Proc Natl Acad Sci U S A 2012;109:E2353–60.
31. Rodriguez J, Vernus B, Toubiana M, Jublanc E, Tintignac L, Leibovitch E, et al. Myostatin inactivation increases myotube size through regulation of translational initiation machinery. J Cell Biochem 2011;112:3531–42.
32. Wang Q, McPherron AC. Myostatin inhibition induces muscle fibre hypertrophy prior to satellite cell activation. J Physiol 2012;9:2151–65.
33. Welle S, Mehta S, Burgess K. Effect of postdevelopmental myostatin depletion on myofibrillar protein metabolism. Am J Physiol Endocrinol Metab 2011;300:E993–1001.
34. Gullett NP, Mazurak VC, Hebbar G, Ziegler TR. Nutritional interventions for cancer-induced cachexia. Curr Probl Cancer 2011;35:58–90.
35. Allen DL, Cleary AS, Lindsay SF, Loh AS, Reed JM. Myostatin expression is increased by food deprivation in a muscle-specific manner and contributes to muscle atrophy during prolonged food deprivation in mice. J Appl Physiol 2010;109:692–701.